Matter-induced charge-symmetry-violating NN potential

Subhrajyoti Biswas, Pradip Roy, and Abhee K. Dutt-Mazumder
Saha Institute of Nuclear Physics, 1/AF Bidhannagar, Kolkata-700 064, India
(Received 12 November 2008; revised manuscript received 5 October 2009; published 19 January 2010)

We construct a density-dependent, Class III, charge-symmetry-violating (CSV) potential due to mixing of the ρ-ω meson with off-shell corrections. Here, in addition to the usual vacuum contribution, the matter-induced mixing of ρ-ω is also included. It is observed that the contribution of the density-dependent CSV potential is comparable to that of the vacuum contribution.

DOI: 10.1103/PhysRevC.81.014006 PACS number(s): 21.65.Cd, 13.75.Cs, 13.75.Gx, 21.30.Fe

I. INTRODUCTION

The exploration of symmetries and their breaking have always been an active and interesting area of research in nuclear physics. One of the well-known examples, which can be cited here, is the nuclear β decay which violates parity that led to the discovery of the weak interaction. Our present concern, however, is the strong interaction where, in particular, we focus attention on the charge-symmetry violation (CSV) in the nucleon-nucleon (NN) interaction.

Charge symmetry implies the invariance of the NN interaction under rotation in isospin space, which in nature is violated. The CSV, at the fundamental level, is caused by the finite mass difference between up (u) and down (d) quarks [1–6]. As a consequence, at the hadronic level, charge symmetry (CS) is violated due to the nondegenerate mass of hadrons of the same isospin multiplet. The general goal of the research in this area is to find small but observable effects of CSV which might provide significant insight into the strong-interaction dynamics.

There are several experimental data which indicate CSV in the NN interaction. For instance, the difference between pp and nn scattering lengths at the ${}^1S_0$ state is nonzero [4,7,8]. Other convincing evidence of CSV comes from the binding-energy difference of mirror nuclei, which is known as the Okamoto-Nolen-Schifer (ONS) anomaly [9–11]. The modern manifestation of CSV includes the difference of neutron-proton form factors, the hadronic correction to $g-2$ [12], the observation of the decay of $\Psi'(3686) \rightarrow (J/\Psi)\pi^0$, etc. [12].

In nuclear physics, one constructs the CSV potential to see its consequences on various observables. The construction of the CSV potential involves evaluating the NN scattering diagrams with intermediate states that include mixing of various isospin states such as ρ-ω or π-η mesons. The former is found to be most dominant [3,13–17], which we consider here.

Most of the calculations performed initially to construct the CSV potential considered the on-shell [16] or constant ρ-ω mixing amplitude [17], which is claimed to be successful in explaining various CSV observables [17,18]. This success has been called into question [19,20] because of the use of the on-shell mixing amplitude for the construction of the CSV potential. First in Ref. [20] and then in Refs. [21–25], it is shown that the ρ-ω mixing has strong momentum dependence, which even changes its sign as one moves away from the ρ (or ω) pole to the space-like region which is relevant for the construction of the CSV potential. Therefore, inclusion of off-shell corrections are necessary for the calculation of CSV potential. We here deal with such a mixing amplitude induced by the N-N loop incorporating off-shell corrections.

In vacuum, the charge symmetry is broken explicitly due to the nondegenerate nucleon masses. In matter, there can be another source of symmetry breaking if the ground state contains unequal numbers of neutrons (n) and protons (p), giving rise to ground-state-induced mixing of various charged states such as the ρ-ω meson, even in the limit $M_n = M_p$. To the best of our knowledge, this additional source of symmetry breaking for the construction of the CSV potential has not been considered before.

The possibility of such matter-induced mixing was first studied in Ref. [26] and was subsequently studied in Refs. [27–30]. For the case of the π-η meson also such asymmetry-driven mixing is studied in Ref. [31]. But none of these studies deal with the construction of a two-body potential, and the calculations are mostly confined to the time-like region where the main motivation is to investigate the role of such matter-induced mixing on the dilepton spectrum observed in heavy-ion collisions, pion form factor, meson dispersion relations, etc. [27,30]. In Ref. [32], an attempt was made to calculate the density-dependent CSV potential by considering only the effect of the scalar mean field on the nucleon mass and excluding the possibility of matter-driven mixing. All existing matter-induced mixing calculations, however, suggest that, at least in the ρ-ω sector, the inclusion of such a matter-induced mixing amplitude into the two-body NN interaction potential can significantly change the results both qualitatively and quantitatively. It is also to be noted that such mixing amplitudes, in asymmetric nuclear matter (ANM), have a nonzero contribution even if the quark or nucleon masses are taken to be equal [26–30]. We consider both of these mechanisms to construct the CSV potential.

Physically, in a dense system, intermediate mesons might be absorbed and re-emitted from the Fermi spheres. In symmetric nuclear matter (SNM), the emission and absorption involving different isospin states like ρ and ω cancel when the contributions of both the proton and neutron Fermi spheres are added, provided the nucleon masses are taken to be equal. In ANM, on the other hand, the unbalanced contributions coming

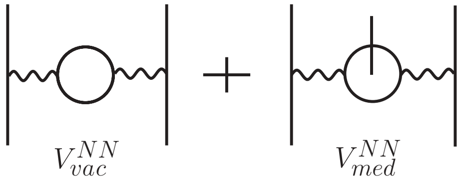

FIG. 1. Feynman diagrams that contribute to the construction of the CSV *NN* potential in matter. Solid lines represent nucleons, and wavy lines stand for vector mesons.

from the scattering of neutron and proton Fermi spheres, lead to the mixing which depends on both the density ρ_B and the asymmetry parameter $\alpha = (\rho_n - \rho_p)/\rho_B$. Inclusion of this process is depicted by the second diagram in Fig. 1 represented by $V_{\rm med}^{NN}$, which is nonzero even in symmetric nuclear matter if explicit mass differences of nucleons are retained. In the first diagram, $V_{\rm vac}^{NN}$ involves a *NN* loop denoted by the circle. The other important element which we include here is the contribution coming from the external legs. This is another source of explicit symmetry violation which significantly modifies the CSV potential in vacuum, as has been shown only recently by the present authors [33].

This paper is organized as follows. In Sec. II we present the formalism where the three-momentum-dependent ρ^0-ω mixing amplitude is calculated to construct the CSV potential in matter. The numerical results are discussed in Sec. III. Finally, we summarize in Sec. IV.

II. FORMALISM

We start with the following effective Lagrangians to describe the ωNN and ρNN interactions:

$$\mathcal{L}_{\omega NN} = g_\omega \bar{\Psi}\gamma_\mu \Phi_\omega^\mu \Psi, \tag{1a}$$

$$\mathcal{L}_{\rho NN} = g_\rho \bar{\Psi}\left[\gamma_\mu + \frac{C_\rho}{2M}\sigma_{\mu\nu}\partial^\mu\right]\vec{\tau}\cdot\Phi_\rho^\nu\Psi, \tag{1b}$$

where $C_\rho = f_\rho/g_\rho$ is the ratio of vector to tensor coupling, M is the average nucleon mass, and $\vec{\tau}$ is the isospin operator. Ψ and Φ represent the nucleon and meson fields, respectively, and g stands for the meson-nucleon coupling constants. The tensor coupling of ω is not included in the present calculation, as it is negligible compared to the vector coupling.

The matrix element, which is required for the construction of the CSV NN potential, is obtained from the relevant Feynman diagram [33]:

$$\mathcal{M}_{\rho\omega}^{NN}(q) = \left[\bar{u}_N(p_3)\Gamma_\rho^\mu(q)u_N(p_1)\right]\Delta_{\mu\alpha}^\rho(q)\Pi_{\rho\omega}^{\alpha\beta}(q^2) \times \Delta_{\beta\nu}^\omega(q)\left[\bar{u}_N(p_4)\Gamma_\omega^\nu(-q)u_N(p_2)\right]. \tag{2}$$

In the limit $q_0 \to 0$, Eq. (2) gives the momentum space CSV NN potential, $V_{\rm CSV}^{NN}(\mathbf{q})$. Here, $\Gamma_\omega^\mu(q) = g_\omega\gamma^\mu$ and $\Gamma_\rho^\nu(q) = g_\rho[\gamma^\nu - \frac{C_\rho}{2M}i\sigma^{\nu\lambda}q_\lambda]$ denote the vertex factors, u_N is the Dirac spinor, and $\Delta_{\mu\nu}^i(q)$ $(i = \rho, \omega)$ is the meson propagator. p_j and q are the four-momenta of the nucleon and meson, respectively.

In the present calculation, the ρ-ω mixing amplitude (i.e., polarization tensor) $\Pi_{\rho\omega}^{\mu\nu}(q^2)$ is generated by the difference between the proton and neutron loop contributions:

$$\Pi_{\rho\omega}^{\mu\nu}(q^2) = \Pi_{\rho\omega}^{\mu\nu(p)}(q^2) - \Pi_{\rho\omega}^{\mu\nu(n)}(q^2). \tag{3}$$

Explicitly, the polarization tensor is given by

$$i\Pi_{\rho\omega}^{\mu\nu(N)}(q^2) = \int\frac{d^4k}{(2\pi)^4}\mathrm{Tr}\left[\Gamma_\omega^\mu(q)G_N(k)\Gamma_\rho^\nu(-q)G_N(k+q)\right], \tag{4}$$

where $k = (k_0, \mathbf{k})$ denotes the four-momentum of the nucleon in the loops (see Fig. 1), and G_N is the in-medium nucleon propagator consisting of free (G_N^F) and density-dependent (G_N^D) parts [34], that is,

$$G_N^F(k) = \frac{\not{k} + M_N}{k^2 - M_N^2 + i\zeta}, \tag{5a}$$

$$G_N^D(k) = \frac{i\pi}{E_N}(\not{k} + M_N)\delta(k_0 - E_N)\theta(k_N - |\mathbf{k}|). \tag{5b}$$

The subscript N stands for the nucleon index (i.e., $N = p$ or n), k_N denotes the Fermi momentum of the nucleon, the nucleon energy $E_N = \sqrt{M_N^2 + k_N^2}$, and the nucleon mass is denoted by M_N. $\theta(k_N - |\mathbf{k}|)$ is the Fermi distribution function at zero temperature.

The origin of $G_N^D(k)$, in addition to the free propagator, stems from the fact that here we are dealing with a vacuum containing real particles for which, when acted upon, the annihilation operator does not vanish (see the Appendix for details). The appearance of the δ function in Eq. (5b) indicates the nucleons are on-shell, while $\theta(k_N - |\mathbf{k}|)$ ensures that propagating nucleons have a momentum less than k_N.

Likewise, the polarization tensor of Eq. (4) also contains a vacuum $[\Pi_{\rm vac}^{\mu\nu(N)}(q^2)]$ and a density-dependent $[\Pi_{\rm med}^{\mu\nu(N)}(q^2)]$ part, as shown in Fig. 1. Note that the density-dependent part given by the combination of $G_N^F G_N^D + G_N^D G_N^F$ corresponds to the scattering that we have discussed already, whereas the term proportional to $G_N^D G_N^D$ vanishes for low energy excitation [35]. The vacuum part $[\Pi_{\rm vac}^{\mu\nu(N)}(q^2)]$, on the other hand, involves $G_N^F G_N^F$, which gives rise to the usual CSV part of the potential due to the splitting of the neutron and proton mass.

It might be worthwhile to mention here that Eq. (5b) can induce charge-symmetry breaking in asymmetric nuclear matter as the result of the appearance of the Fermi distribution function in the propagator itself, which can distinguish between neutron and proton, even if their masses are taken to be degenerate. Evidently, this is an exclusive medium-driven effect where, as mentioned already in the Introduction, the charge symmetry is broken by the ground state. The total charge-symmetry breaking would involve both contributions, where it is clear that even for $\alpha = 0$, the medium-dependent term can contribute if the nondegenerate nucleon masses are considered.

Note that the polarization tensor $\Pi_{\rho\omega}^{\mu\nu}(q^2)$ can be expressed as the sum of the longitudinal component $\Pi_{\rho\omega}^L(q^2)$ and the transverse component $\Pi_{\rho\omega}^T(q^2)$, which is useful for simplifying the matrix element given in Eq. (2), i.e.,

$$\Pi_{\rho\omega}^{\mu\nu}(q^2) = \Pi_{\rho\omega}^L(q^2)A^{\mu\nu} + \Pi_{\rho\omega}^T(q^2)B^{\mu\nu}, \tag{6}$$

where $A^{\mu\nu}$ and $B^{\mu\nu}$ are the longitudinal and transverse projection operators [36]. We define $\Pi^L_{\rho\omega} = -\Pi^{00}_{\rho\omega} + \Pi^{33}_{\rho\omega}$ and $\Pi^T_{\rho\omega} = \Pi^{11}_{\rho\omega} = \Pi^{22}_{\rho\omega}$.

In the present calculation, we use the average of the longitudinal and transverse components of the polarization tensor instead of $\Pi^L_{\rho\omega}$ and $\Pi^T_{\rho\omega}$. The average mixing amplitude is denoted by

$$\bar{\Pi}(q^2) = \tfrac{1}{3}\left[\Pi^L_{\rho\omega}(q^2) + 2\Pi^T_{\rho\omega}(q^2)\right] = \bar{\Pi}_{\rm vac}(q^2) + \bar{\Pi}_{\rm med}(q^2). \tag{7}$$

In the last line of Eq. (7), $\bar{\Pi}_{\rm vac}(q^2)$ and $\bar{\Pi}_{\rm med}(q^2)$ denote the average mixing amplitudes of the vacuum and density-dependent parts, respectively.

To obtain $\bar{\Pi}_{\rm vac}(q^2)$ and $\bar{\Pi}_{\rm med}(q^2)$ one would calculate the total polarization tensor given in Eq. (4). After evaluating the trace of Eq. (4), we find the following vacuum and density-dependent parts of the polarization tensor:

$$\Pi^{\mu\nu(N)}_{\rm vac}(q^2) = Q^{\mu\nu}\left[\Pi^{{\rm vv}(N)}_{\rm vac}(q^2) + \Pi^{{\rm tv}(N)}_{\rm vac}(q^2)\right], \tag{8}$$

and

$$\Pi^{\mu\nu\{{\rm vv}(N)\}}_{\rm med}(q^2) = 16 g_\rho g_\omega \int \frac{d^3k}{(2\pi)^3 2E_N}\theta(k_N - |\mathbf{k}|) \times \frac{q^2 K^{\mu\nu} - (q\cdot k)^2 Q^{\mu\nu}}{q^4 - 4(q\cdot k)^2}, \tag{9}$$

$$\Pi^{\mu\nu\{{\rm tv}(N)\}}_{\rm med}(q^2) = 4 g_\rho g_\omega C_\rho \int \frac{d^3k}{(2\pi)^3 2E_N}\theta(k_N - |\mathbf{k}|) \times \frac{q^4 Q^{\mu\nu}}{q^4 - 4(q\cdot k)^2}, \tag{10}$$

where $Q^{\mu\nu} = -g^{\mu\nu} + q^\mu q^\nu/q^2$ and $K^{\mu\nu} = (k^\mu - (q\cdot k)\frac{q^\mu}{q^2})(k^\nu - (q\cdot k)\frac{q^\nu}{q^2})$. Note that both $\Pi^{\mu\nu}_{\rm vac}(q^2)$ and $\Pi^{\mu\nu}_{\rm med}(q^2)$ obey the current conservation as $q_\mu Q^{\mu\nu} = q_\nu Q^{\mu\nu} = 0$ and $q_\mu K^{\mu\nu} = q_\nu K^{\mu\nu} = 0$. The superscripts vv and tv in Eqs. (8)–(10) indicate the vector-vector and tensor-vector interactions, respectively. The dimensional counting shows that the vacuum part of the polarization tensor [both $\Pi^{{\rm vv}(N)}_{\rm vac}(q^2)$ and $\Pi^{{\rm tv}(N)}_{\rm vac}(q^2)$] is ultraviolet divergent, and dimensional regularization [37–39] is used to isolate the divergent parts. Since the mixing amplitude is generated by the difference between the proton and neutron loop contributions, the divergent parts cancel out, yielding the vacuum amplitude finite.

$$\Pi^{\mu\nu}_{\rm vac}(q^2) = \Pi^{\mu\nu(p)}_{\rm vac}(q^2) - \Pi^{\mu\nu(n)}_{\rm vac}(q^2) = \frac{g_\rho g_\omega}{2\pi^2} q^2 Q^{\mu\nu} \int_0^1 dx\left((1-x)x + \frac{C_\rho}{4}\right) \times \ln\left(\frac{M_p^2 - x(1-x)q^2}{M_n^2 - x(1-x)q^2}\right). \tag{11}$$

Equation (11) shows the four-momentum-dependent vacuum polarization tensor. From this equation, one can calculate the longitudinal ($\Pi^L_{\rm vac}$) and transverse ($\Pi^T_{\rm vac}$) components of the vacuum mixing amplitude, and in the limit $q_0 \to 0$, $\Pi^L_{\rm vac}(\mathbf{q}^2) = \Pi^T_{\rm vac}(\mathbf{q}^2)$. Therefore, the average vacuum mixing amplitude is

$$\bar{\Pi}_{\rm vac}(\mathbf{q}^2) = \frac{1}{3}\left[\Pi^L_{\rm vac}(\mathbf{q}^2) + 2\Pi^T_{\rm vac}(\mathbf{q}^2)\right] = -\frac{g_\rho g_\omega}{12\pi^2}(2 + 3C_\rho)\ln\left(\frac{M_p}{M_n}\right)\mathbf{q}^2 \equiv -\mathcal{A}\mathbf{q}^2. \tag{12}$$

Equation (12) represents the three-momentum-dependent vacuum mixing amplitude. This mixing amplitude vanishes for $M_n = M_p$, and then no CSV potential in vacuum will exist.

To calculate the density-dependent mixing amplitude from Eqs. (9) and (10), we consider $E_N \approx M_N$. In the limit $q_0 \to 0$, one finds the expressions

$$\Pi^{00(N)}_{\rm med}(\mathbf{q}^2) = -\frac{g_\rho g_\omega}{4\pi^2 M_N}\left\{\left[\frac{4}{3}k_N^3 - \frac{1}{2}k_N\mathbf{q}^2 + 2k_N M_N^2 - \left(\frac{\mathbf{q}^3}{8} - \frac{\mathbf{q}k_N^2}{2} - \frac{\mathbf{q}M_N^2}{2} + 2\frac{M_N^2 k_N^2}{\mathbf{q}}\right) \times \ln\left(\frac{\mathbf{q} - 2k_N}{\mathbf{q} + 2k_N}\right)\right] + \frac{C_\rho}{2}\left[\mathbf{q}^2 k_N + \left(\frac{\mathbf{q}^3}{4} - \mathbf{q}k_N^2\right)\ln\left(\frac{\mathbf{q} - 2k_N}{\mathbf{q} + 2k_N}\right)\right]\right\}, \tag{13}$$

$$\Pi^{11(N)}_{\rm med}(\mathbf{q}^2) = \frac{g_\rho g_\omega}{4\pi^2 M_N}\left\{\left[\frac{1}{3}k_N^3 - \frac{3}{8}\mathbf{q}^2 k_N - \left(\frac{3}{32}\mathbf{q}^3 + \frac{k_N^4}{2\mathbf{q}} + \frac{\mathbf{q}^2 k_N}{4}\right) \times \ln\left(\frac{\mathbf{q} - 2k_N}{\mathbf{q} + 2k_N}\right)\right] + \frac{C_\rho}{2}\left[\mathbf{q}^2 k_N + \left(\frac{\mathbf{q}^3}{4} - \mathbf{q}k_N^2\right)\ln\left(\frac{\mathbf{q} - 2k_N}{\mathbf{q} + 2k_N}\right)\right]\right\}. \tag{14}$$

Note that the terms within the first square brackets of both Eqs. (13) and (14) arise from the vector-vector interaction, while the terms within the second square brackets arise from the tensor-vector interaction of the density-dependent polarization tensor. The 33 component of the density-dependent polarization tensor vanishes, i.e., $\Pi^{33(N)}_{\rm med}(\mathbf{q}^2) = 0$. Now

$$\bar{\Pi}_{\rm med}(\mathbf{q}^2) = \tfrac{1}{3}\left[\Pi^L_{\rm med}(\mathbf{q}^2) + 2\Pi^T_{\rm med}(\mathbf{q}^2)\right], \tag{15}$$

where

$$\Pi^L_{\rm med}(\mathbf{q}^2) = -\left[\Pi^{00(p)}_{\rm med}(\mathbf{q}^2) - \Pi^{00(n)}_{\rm med}(\mathbf{q}^2)\right], \tag{16}$$

$$\Pi^T_{\rm med}(\mathbf{q}^2) = -\left[\Pi^{11(p)}_{\rm med}(\mathbf{q}^2) - \Pi^{11(n)}_{\rm med}(\mathbf{q}^2)\right]. \tag{17}$$

With the suitable expansion of Eqs. (13) and (14) in terms of $|\mathbf{q}|/k_{p(n)}$ and keeping $\mathcal{O}(\mathbf{q}^2/k^2_{p(n)})$ terms, we get

$$\bar{\Pi}_{\rm med}(\mathbf{q}^2) \simeq \Delta' - \mathcal{A}'\mathbf{q}^2, \tag{18}$$

where

$$\Delta' = \frac{g_\rho g_\omega}{12\pi^2}\left[3\left(\frac{k_p^3}{M_P} - \frac{k_n^3}{M_n}\right) + 4(k_p M_p - k_n M_n)\right], \tag{19}$$

$$\mathcal{A}' = \frac{g_\rho g_\omega}{12\pi^2}\left[3(1 - C_\rho)\left(\frac{k_p}{M_p} - \frac{k_n}{M_n}\right) + \frac{1}{3}\left(\frac{M_p}{k_p} - \frac{M_n}{k_n}\right)\right]. \tag{20}$$

Clearly, $\bar{\Pi}_{\rm med}(\mathbf{q}^2)$ is also three-momentum dependent; and if $M_n = M_p$, it vanishes in SNM but is nonvanishing in ANM. In the present calculation, nucleon masses are considered nondegenerate and the asymmetry parameter $\alpha \neq 0$.

To construct the CSV potential, we take the nonrelativistic (NR) limit of the Dirac spinors, in which case we obtain

$$u_N(\mathbf{p}) \simeq \left(1 - \frac{\mathbf{P}^2}{8M_N^2} - \frac{\mathbf{q}^2}{32M_N^2}\right)\begin{pmatrix} 1 \\ \frac{\sigma\cdot(\mathbf{P}+\mathbf{q}/2)}{2M_N}\end{pmatrix}, \tag{21}$$

where σ is the spin of the nucleon. $\mathbf{P}$ denotes the average three-momentum of the interacting nucleon pair, and $\mathbf{q}$ stands for the three-momentum of the meson.

The explicit expression of the full CSV potential in momentum space can be obtained from Eq. (13) of Ref. [33] by replacing the mixing amplitude $\Pi_{\rho\omega}(\mathbf{q})$ with $\bar{\Pi}(\mathbf{q}^2)$.

$$\begin{aligned} V_{\rm CSV}^{NN}(\mathbf{q}) = &-\frac{g_\rho g_\omega \bar{\Pi}(\mathbf{q}^2)}{(\mathbf{q}^2+m_\rho^2)(\mathbf{q}^2+m_\omega^2)} \\ &\times\Bigg\{T_3^+\Bigg[\left(1+\frac{3\mathbf{P}^2}{2M_N^2}-\frac{\mathbf{q}^2}{8M_N^2}-\frac{\mathbf{q}^2}{4M_N^2}(\sigma_1\cdot\sigma_2)\right. \\ &+\frac{3i}{2M_N^2}\mathbf{S}\cdot(\mathbf{q}\times\mathbf{P})+\frac{1}{4M_N^2}(\sigma_1\cdot\mathbf{q})(\sigma_2\cdot\mathbf{q}) \\ &\left.+\frac{1}{M_N^2}(\hat{\mathbf{q}}\cdot\mathbf{P})^2\right)-\frac{C_\rho}{2M}\left(\frac{\mathbf{q}^2}{2M_N}+\frac{\mathbf{q}^2}{2M_N}(\sigma_1\cdot\sigma_2)\right. \\ &\left.-\frac{2i}{M_N}\mathbf{S}\cdot(\mathbf{q}\times\mathbf{P})-\frac{1}{2M_N}(\sigma_1\cdot\mathbf{q})(\sigma_2\cdot\mathbf{q})\right)\Bigg] \\ &-T_3^-\frac{C_\rho}{2M}\Bigg[\left(\frac{\mathbf{q}^2}{2M}-\frac{\mathbf{q}^2}{2M}(\sigma_1\cdot\sigma_2)\right. \\ &\left.+\frac{1}{2M}(\sigma_1\cdot\mathbf{q})(\sigma_2\cdot\mathbf{q})\right)\frac{\Delta M(1,2)}{M} \\ &-\frac{i}{M}(\sigma_1-\sigma_2)\cdot(\mathbf{q}\times\mathbf{P})\Bigg]\Bigg\}. \end{aligned} \tag{22}$$

Equation (22) presents the full CSV NN potential in momentum space in matter. Here, $T_3^{\pm} = \tau_3(1) \pm \tau_3(2)$ and $\mathbf{S} = \frac{1}{2}(\sigma_1+\sigma_2)$ is the total spin of the interacting nucleon pair. We define $M = (M_n + M_p)/2$, $\Delta M = (M_n - M_p)/2$, and $\Delta M(1,2) = -\Delta M(2,1) = \Delta M$. It is be mentioned that the spin-dependent parts of the potential appear because of the contribution of the external nucleon legs shown in Fig. 1. On the other hand, $3\mathbf{P}^2/2M_N^2$ and $-\mathbf{q}^2/8M_N^2$ arise because of the expansion of the relativistic energy E_N of the spinors.

In matter, $V_{\rm CSV}^{NN}(\mathbf{q})$ consists of two parts: one contains the vacuum mixing amplitude and the other contains the density-dependent mixing amplitude. The former is denoted by $V_{\rm vac}^{NN}(\mathbf{q})$, and latter by $V_{\rm med}^{NN}(\mathbf{q})$. Thus, $V_{\rm CSV}^{NN}(\mathbf{q}) = V_{\rm vac}^{NN}(\mathbf{q}) + V_{\rm med}^{NN}(\mathbf{q})$.

From Eq. (22), we extract the following term, which in coordinate space gives rise to the δ-function potential:

$$\delta V_{\rm CSV}^{NN} = g_\rho g_\omega(\mathcal{A}+\mathcal{A}')\left[\left(\frac{1+2C_\rho}{8M_N^2}\right)+\left(\frac{1+C_\rho}{4M_N^2}\right)(\sigma_1\cdot\sigma_2)\right]. \tag{23}$$

To avoid the appearance of the δ-function potential in coordinate space, one should introduce form factors $F_i(\mathbf{q}^2)$, for which the meson-nucleon coupling constants become momentum-dependent, i.e., $g_i(\mathbf{q}^2) = g_i F_i(\mathbf{q}^2)$. Here we use the following form factor:

$$F_i(\mathbf{q}^2) = \frac{\Lambda_i^2 - m_i^2}{\Lambda_i^2 + \mathbf{q}^2}, \tag{24}$$

where Λ_i is the cutoff parameter governing the range of the suppression, and m_i denotes the mass of exchanged meson.

The full CSV potential presented in Eq. (22) contains both Class III and Class IV potentials, and both break the charge symmetry in NN interactions. The terms within the first and the second square brackets represent Class III and Class IV potentials, respectively. The Class III potential differentiates between nn and pp systems, while the Class IV NN potential exists in the np system only. In this paper, we restrict ourselves to the Class III potential only.

The coordinate space potential can be easily obtained by Fourier transformation of $V_{\rm CSV}^{NN}(\mathbf{q})$, i.e.,

$$V_{\rm CSV}^{NN}(\mathbf{r}) = \int \frac{d^3\mathbf{q}}{(2\pi)^3} V_{\rm CSV}^{NN}(\mathbf{q}) e^{-i\mathbf{q}\cdot\mathbf{r}}. \tag{25}$$

We drop the term $3\mathbf{P}^2/2M_N^2$ from Eq. (22) while taking the Fourier transform, as it is not important in the present context. However, this term becomes important to fitting ${}^1S_0$ and ${}^3P_2$ phase shifts simultaneously.

Now the CSV potential in coordinate space without $\delta V_{\rm CSV}^{NN}$ reduces to

$$\begin{aligned} V_{\rm vac}^{NN}(\mathbf{r}) = &-\frac{g_\rho g_\omega}{4\pi}\mathcal{A}T_3^+\Bigg[\left(\frac{m_\rho^3 Y_0(x_\rho) - m_\omega^3 Y_0(x_\omega)}{m_\omega^2 - m_\rho^2}\right) \\ &+\frac{1}{M_N^2}\left(\frac{m_\rho^5 V_{\rm vv}(x_\rho) - m_\omega^3 V_{\rm vv}(x_\omega)}{m_\omega^2 - m_\rho^2}\right) \\ &+\frac{C_\rho}{2M_N^2}\left(\frac{m_\rho^5 V_{\rm tv}(x_\rho) - m_\omega^3 V_{\rm tv}(x_\omega)}{m_\omega^2 - m_\rho^2}\right)\Bigg], \end{aligned} \tag{26}$$

$$\begin{aligned} V_{\rm med}^{NN}(\mathbf{r}) = &-\frac{g_\rho g_\omega}{4\pi}T_3^+\Bigg\{\Delta'\Bigg[\left(\frac{m_\rho Y_0(x_\rho) - m_\omega Y_0(x_\omega)}{m_\omega^2 - m_\rho^2}\right) \\ &+\frac{1}{M_N^2}\left(\frac{m_\rho^3 V_{\rm vv}(x_\rho) - m_\omega^3 V_{\rm vv}(x_\omega)}{m_\omega^2 - m_\rho^2}\right) \\ &+\frac{C_\rho}{2M_N^2}\left(\frac{m_\rho^3 V_{\rm tv}(x_\rho) - m_\omega^3 V_{\rm tv}(x_\omega)}{m_\omega^2 - m_\rho^2}\right)\Bigg] \\ &+\mathcal{A}'\Bigg[\left(\frac{m_\rho^3 Y_0(x_\rho) - m_\omega^3 Y_0(x_\omega)}{m_\omega^2 - m_\rho^2}\right) \\ &+\frac{1}{M_N^2}\left(\frac{m_\rho^5 V_{\rm vv}(x_\rho) - m_\omega^5 V_{\rm vv}(x_\omega)}{m_\omega^2 - m_\rho^2}\right) \\ &+\frac{C_\rho}{2M_N^2}\left(\frac{m_\rho^5 V_{\rm tv}(x_\rho) - m_\omega^5 V_{\rm tv}(x_\omega)}{m_\omega^2 - m_\rho^2}\right)\Bigg]\Bigg\}, \end{aligned} \tag{27}$$

where $x_i = m_i r$. The explicit expressions of $V_{\rm vv}(x_i)$ and $V_{\rm tv}(x_i)$ are given in Ref. [33]. In Eqs. (26) and (27), the M_N^{-2} independent terms represent central parts without contributions of external nucleon legs.

The potentials presented in Eqs. (26) and (27) do not include the form factors, so these potentials diverge near the core. The problem of divergence near the core can be removed by incorporating form factors as discussed before. With the inclusion of form factors, $V_{\rm vac}^{NN}(\mathbf{r})$ and $V_{\rm med}^{NN}(\mathbf{r})$ take the form

$$\begin{aligned}V_{\rm vac}^{NN}(\mathbf{r}) = -\frac{g_\rho g_\omega}{4\pi}\mathcal{A}T_3^+\Bigg\{&\left(\frac{a_\rho m_\rho^3 Y_0(x_\rho) - a_\omega m_\omega^3 Y_0(x_\omega)}{m_\omega^2 - m_\rho^2}\right)\\&+\frac{1}{M_N^2}\left(\frac{a_\rho m_\rho^5 V_{\rm vv}(x_\rho) - a_\omega m_\omega^5 V_{\rm vv}(x_\omega)}{m_\omega^2 - m_\rho^2}\right)\\&+\frac{C_\rho}{2M_N^2}\left(\frac{a_\rho m_\rho^5 V_{\rm tv}(x_\rho) - a_\omega m_\omega^5 V_{\rm tv}(x_\omega)}{m_\omega^2 - m_\rho^2}\right)\\&-\lambda\Bigg[\left(\frac{b_\rho \Lambda_\rho^3 Y_0(X_\rho) - b_\omega \Lambda_\omega^3 Y_0(X_\omega)}{m_\omega^2 - m_\rho^2}\right)\\&+\frac{1}{M_N^2}\left(\frac{b_\rho \Lambda_\rho^5 V_{\rm vv}(X_\rho) - b_\omega \Lambda_\omega^5 V_{\rm vv}(X_\omega)}{m_\omega^2 - m_\rho^2}\right)\\&+\frac{C_\rho}{2M_N^2}\left(\frac{b_\rho \Lambda_\rho^5 V_{\rm tv}(X_\rho) - b_\omega \Lambda_\omega^5 V_{\rm tv}(X_\omega)}{m_\omega^2 - m_\rho^2}\right)\Bigg]\Bigg\},\end{aligned} \tag{28}$$

$$\begin{aligned}V_{\rm med}^{NN}(\mathbf{r}) = -\frac{g_\rho g_\omega}{4\pi}T_3^+\Bigg\{&\Delta'\Bigg[\left(\frac{a_\rho m_\rho Y_0(x_\rho) - a_\omega m_\omega Y_0(x_\omega)}{m_\omega^2 - m_\rho^2}\right)\\&+\frac{1}{M_N^2}\left(\frac{a_\rho m_\rho^3 V_{\rm vv}(x_\rho) - a_\omega m_\omega^3 V_{\rm vv}(x_\omega)}{m_\omega^2 - m_\rho^2}\right)\\&+\frac{C_\rho}{2M_N^2}\left(\frac{a_\rho m_\rho^3 V_{\rm tv}(x_\rho) - a_\omega m_\omega^3 V_{\rm tv}(x_\omega)}{m_\omega^2 - m_\rho^2}\right)\Bigg]\\&+\mathcal{A}'\Bigg[\left(\frac{a_\rho m_\rho^3 Y_0(x_\rho) - a_\omega^3 m_\omega Y_0(x_\omega)}{m_\omega^2 - m_\rho^2}\right)\\&+\frac{1}{M_N^2}\left(\frac{a_\rho m_\rho^5 V_{\rm vv}(x_\rho) - a_\omega m_\omega^5 V_{\rm vv}(x_\omega)}{m_\omega^2 - m_\rho^2}\right)\\&+\frac{C_\rho}{2M_N^2}\left(\frac{a_\rho m_\rho^5 V_{\rm tv}(x_\rho) - a_\omega m_\omega^5 V_{\rm tv}(x_\omega)}{m_\omega^2 - m_\rho^2}\right)\Bigg]\\&-\lambda\Delta'\Bigg[\left(\frac{b_\rho \Lambda_\rho Y_0(X_\rho) - b_\omega \Lambda_\omega Y_0(X_\omega)}{m_\omega^2 - m_\rho^2}\right)\\&+\frac{1}{M_N^2}\left(\frac{b_\rho \Lambda_\rho^3 V_{\rm vv}(X_\rho) - b_\omega \Lambda_\omega^3 V_{\rm vv}(X_\omega)}{m_\omega^2 - m_\rho^2}\right)\\&+\frac{C_\rho}{2M_N^2}\left(\frac{b_\rho \Lambda_\rho^3 V_{\rm tv}(X_\rho) - b_\omega \Lambda_\omega^3 V_{\rm tv}(X_\omega)}{m_\omega^2 - m_\rho^2}\right)\Bigg]\\&-\lambda\mathcal{A}'\Bigg[\left(\frac{b_\rho \Lambda_\rho^3 Y_0(X_\rho) - b_\omega \Lambda_\omega^3 Y_0(X_\omega)}{m_\omega^2 - m_\rho^2}\right)\\&+\frac{1}{M_N^2}\left(\frac{b_\rho \Lambda_\rho^5 V_{\rm vv}(X_\rho) - b_\omega \Lambda_\omega^5 V_{\rm vv}(X_\omega)}{m_\omega^2 - m_\rho^2}\right)\\&+\frac{C_\rho}{2M_N^2}\left(\frac{b_\rho \Lambda_\rho^5 V_{\rm tv}(X_\rho) - b_\omega \Lambda_\omega^5 V_{\rm tv}(X_\omega)}{m_\omega^2 - m_\rho^2}\right)\Bigg]\Bigg\}.\end{aligned} \tag{29}$$

In Eqs. (28) and (29), $X_i = \Lambda_i r$, and

$$\lambda = \frac{m_\omega^2 - m_\rho^2}{\Lambda_\omega^2 - \Lambda_\rho^2}, \tag{30}$$

$$a_i = \frac{\Lambda_j^2 - m_j^2}{\Lambda_j^2 - m_i^2}, \quad b_i = \frac{\Lambda_j^2 - m_j^2}{m_j^2 - \Lambda_i^2}, \quad \text{where } i(j) = \rho, \quad \omega\ (i \neq j). \tag{31}$$

Note that Eqs. (28) and (29) contain the contribution of $\delta V_{\rm CSV}^{NN}$, and the problem of divergence near the core is removed.

III. RESULTS

Using Eqs. (26) and (27), we show in Fig. 2 the difference of CSV potentials between nn and pp systems, i.e., $\Delta V = V_{\rm CSV}^{nn} - V_{\rm CSV}^{pp}$ for the $^1S_0$ state at nuclear matter density $\rho_B = 0.148$ fm^{-3} with asymmetry parameter $\alpha = 1/3$. The dashed and dotted curves show $\Delta V_{\rm vac}$ and $\Delta V_{\rm med}$, respectively. The total contribution (i.e., $\Delta V_{\rm vac} + \Delta V_{\rm med}$) is shown by the solid curve. It is observed that the density-dependent CSV potential cannot be neglected while estimating CSV observables such as the binding-energy difference of mirror nuclei.

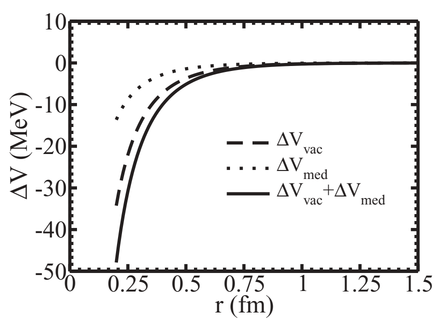

FIG. 2. ΔV for the $^1S_0$ state without $\delta V_{\rm CSV}^{NN}$ and form factors at $\rho_B = 0.148$ fm^{-3} and $\alpha = 1/3$.

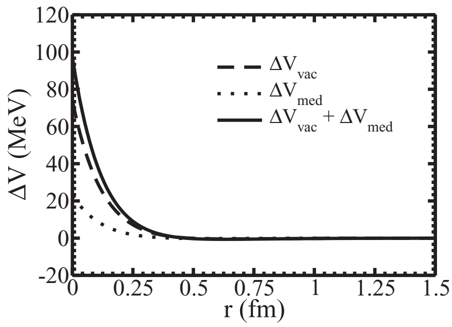

FIG. 3. Same as Fig. 2, but with form factors including the Fourier transform of $\delta V_{\rm CSV}^{NN}$.

Figure 3 displays ΔV for the ${}^1S_0$ state including the Fourier transform of $\delta V_{\rm CSV}^{NN}$ and form factors. Note that incorporating the form factors removes the problem of divergence near the core. Also, the CSV NN potential changes its sign due to the inclusion of the Fourier transform of $\delta V_{\rm CSV}^{NN}$.

IV. SUMMARY AND DISCUSSION

In this work, we have constructed the CSV NN potential in dense matter using an asymmetry-driven momentum-dependent ρ^0-ω mixing amplitude within the framework of the one-boson exchange model. Furthermore, the correction to the central part of the CSV potential due to external nucleon legs is also considered. The closed-form analytic expressions both for vacuum and density-dependent CSV NN potentials in coordinate space are presented.

We have shown that the vacuum mixing amplitude and the density-dependent mixing amplitude are of similar order of magnitude and both contribute with the same sign to the CSV potential. The contribution of the density-dependent CSV potential is not negligible in comparison to the vacuum CSV potential.

APPENDIX

The position space fermion propagator in vacuum is given by the vacuum expectation value of the time-ordered product of fermion fields:

$$i\tilde{G}_N(x-x') = \langle 0|\mathcal{T}[\psi(x)\bar{\psi}(x')]|0\rangle\,. \tag{A1}$$

In a medium, the vacuum $|0\rangle$ is replaced by the ground state $|\Psi_0\rangle$ which contains positive-energy particles with the same Fermi momentum k_N and no antiparticles. Thus,

$$\begin{aligned} i\tilde{G}_N(x-x') &= \langle\Psi_0|\psi(x)\bar{\psi}(x')|\Psi_0\rangle\,\theta(t-t') \\ &\quad - \langle\Psi_0|\bar{\psi}(x')\psi(x)|\Psi_0\rangle\,\theta(t'-t). \end{aligned} \tag{A2}$$

Note that the time-ordered product in Eq. (A2) involves a negative sign for fermions. The fermion field contains both the positive- and negative-energy solutions. The modal expansions for the fermion fields are

$$\psi(x) = \int \frac{d^3\mathbf{k}}{\sqrt{(2\pi)^3 2E_k}} \sum_s (a_{ks}u_{ks}\,e^{-ik\cdot x} + b_{ks}^\dagger v_{ks}\,e^{ik\cdot x}), \tag{A3}$$

$$\bar{\psi}(x) = \int \frac{d^3\mathbf{k}}{\sqrt{(2\pi)^3 2E_k}} \sum_s (a_{ks}^\dagger \bar{u}_{ks}\,e^{ik\cdot x} + b_{ks}\bar{v}_{ks}\,e^{-ik\cdot x}). \tag{A4}$$

Here, $a_{ks}^\dagger$ and a_{ks} are the creation and annihilation operators for particles, and likewise $b_{ks}^\dagger$ and b_{ks} are the creation and annihilation operators for antiparticles. The only nonvanishing anticommutation relations are

$$\{a_{ks}, a_{k's'}^\dagger\} = \{b_{ks}, b_{k's'}^\dagger\} = \delta_{ss'}\delta^3(\mathbf{k}-\mathbf{k}'). \tag{A5}$$

Since $|\Psi_0\rangle$ contains only positive-energy particles, we have the following relations:

$$\begin{aligned} b_{ks}|\Psi_0\rangle &= 0 \quad \text{for all} \quad \mathbf{k}, \\ a_{ks}|\Psi_0\rangle &= 0 \quad \text{for} \quad |\mathbf{k}| > k_N, \\ a_{ks}^\dagger|\Psi_0\rangle &= 0 \quad \text{for} \quad |\mathbf{k}| < k_N, \\ a_{ks}a_{ks}^\dagger|\Psi_0\rangle &= n(\mathbf{k})|\Psi_0\rangle, \end{aligned} \tag{A6}$$

where $n(\mathbf{k})$ is either 0 or 1, and this can be accomplished with the step function $\theta(k_N - |\mathbf{k}|)$. Using Eqs. (A3)–(A6), one obtains

$$\begin{aligned} &\langle\Psi_0|\psi(x)\bar{\psi}(x')|\Psi_0\rangle \\ &= \int \frac{d^3\mathbf{k}}{\sqrt{(2\pi)^3 2E_k}} \int \frac{d^3\mathbf{k}'}{\sqrt{(2\pi)^3 2E_{k'}}} \\ &\quad \times \sum_{ss'} \langle\Psi_0|a_{ks}a_{k's'}^\dagger|\Psi_0\rangle u_{ks}\bar{u}_{k's'}\,e^{-i(k\cdot x - k'\cdot x')} \\ &= \int \frac{d^3\mathbf{k}}{(2\pi)^3 2E_k} (\not{k} + M_N)\,e^{-ik\cdot(x-x')}[1-\theta(k_N - |\mathbf{k}|)], \end{aligned} \tag{A7}$$

and

$$\begin{aligned} &\langle\Psi_0|\bar{\psi}(x')\psi(x)|\Psi_0\rangle \\ &= \int \frac{d^3\mathbf{k}}{\sqrt{(2\pi)^3 2E_k}} \int \frac{d^3\mathbf{k}'}{\sqrt{(2\pi)^3 2E_{k'}}} \\ &\quad \times \sum_{ss'} [\langle\Psi_0|a_{k's'}^\dagger a_{ks}|\Psi_0\rangle \bar{u}_{k's'}u_{ks}\,e^{-i(k\cdot x - k'\cdot x')} \\ &\quad + \langle\Psi_0|b_{k's'}b_{ks}^\dagger|\Psi_0\rangle \bar{v}_{k's'}v_{ks}e^{i(k\cdot x - k'\cdot x')}] \\ &= \int \frac{d^3\mathbf{k}}{(2\pi)^3 2E_k} [(\not{k} + M_N)\,e^{-ik\cdot(x-x')}\theta(k_N - |\mathbf{k}|) \\ &\quad + (\not{k} - M_N)\,e^{ik\cdot(x-x')}]. \end{aligned} \tag{A8}$$

Now,

$$\theta(t-t')e^{-ik\cdot(x-x')} = i\int \frac{dk_0}{2\pi} \frac{e^{-ik\cdot(x-x')}}{k_0 - E_k + i\epsilon}, \tag{A9}$$

$$\theta(t'-t)e^{-ik\cdot(x-x')} = -i\int \frac{dk_0}{2\pi} \frac{e^{-ik\cdot(x-x')}}{k_0 - E_k - i\epsilon}, \tag{A10}$$

$$\theta(t'-t)e^{ik\cdot(x-x')} = i\int \frac{dk_0}{2\pi} \frac{e^{ik\cdot(x-x)}}{k_0 - E_k + i\epsilon}. \tag{A11}$$

From Eqs. (A8), (A10), and (A11), we have

$$\begin{aligned}\langle\Psi_0|\bar{\psi}(x')\psi(x)|\Psi_0\rangle\theta(t-t')\\ &= -i\int\frac{d^4k}{(2\pi)^4 2E_k}e^{-ik\cdot(x-x')}(\not{k}+M_N)\frac{\theta(k_N-|\mathbf{k}|)}{k_0-E_k-i\epsilon}\\ &\quad + i\int\frac{d^4k}{(2\pi)^4 2E_k}(\not{k}-M_N)\frac{e^{ik\cdot(x-x')}}{k_0-E_k+i\epsilon}. \qquad (A12)\end{aligned}$$

Now changing $k\to -k$ in the last integral of Eq. (A12) and substituting Eqs. (A7), (A9), and (A12) in Eq. (A2), we get

$$\begin{aligned} i\tilde{G}_N(x-x')\\ &= i\int\frac{d^4k}{(2\pi)^4 2E_N}e^{-ik\cdot(x-x')}(\not{k}+M_N)\\ &\quad\times\left(\frac{1-\theta(k_N-|\mathbf{k}|)}{k_0-E_N+i\epsilon}+\frac{\theta(k_N-|\mathbf{k}|)}{k_0-E_N-i\epsilon}-\frac{1}{k_0+E_N-i\epsilon}\right). \qquad (A13)\end{aligned}$$

In Eq. (A13), E_k has been replaced by E_N. The first term of Eq. (A13) represents particle propagation above the Fermi sea, and the second term indicates the propagation of holes inside the Fermi sea. The last term shows the propagation of holes in the infinite Dirac sea. Now,

$$\frac{1}{k_0-E_N+i\epsilon}-\frac{1}{k_0+E_N-i\epsilon}=\frac{2E_N}{k^2-M_N^2+i\zeta}, \qquad (A14)$$

$$\frac{1}{k_0-E_N-i\epsilon}-\frac{1}{k_0-E_N+i\epsilon}=2i\pi\delta(k_0-E_N). \qquad (A15)$$

From Eqs. (A13)–(A15),

$$i\tilde{G}_N(x-x')=i\int\frac{d^4k}{(2\pi)^4}e^{-ik\cdot(x-x')}G_N(k), \qquad (A16)$$

where $G_N(k)$ is the in-medium fermion propagator in momentum space, i.e.,

$$\begin{aligned}G_N(k) &= \frac{\not{k}+M_N}{k^2-M_N^2+i\epsilon}+\frac{i\pi}{E_N}(\not{k}+M_N)\delta(k_0-E_N)\theta(k_N-|\mathbf{k}|)\\ &= G_N^F(k)+G_N^D(k). \qquad (A17)\end{aligned}$$

[1] J. A. Nolen and J. P. Schiffer, Annu. Rev. Nucl. Sci. **19**, 471 (1969).
[2] E. M. Henley, in *Isospin in Nuclear Physics*, edited by D. H. Wilkinson (North-Holland, Amsterdam, 1969), p. 17.
[3] E. M. Henley and G. A. Miller, in *Mesons in Nuclei*, edited by M. Rho and D. H. Wilkinson (North-Holland, Amsterdam, 1979), p. 405.
[4] G. A. Miller, M. K. Nefkens, and I. Slaus, Phys. Rep. **194**, 1 (1990).
[5] R. Machleidt, Adv. Nucl. Phys. **19**, 189 (1989).
[6] G. A. Miller and W. H. T. van Oers, in *Symmetries and Fundamental Interactions in Nuclei*, edited by W. C. Haxton and E. M. Henley (World Scientific, Singapore, 1995), p. 127.
[7] C. R. Howell *et al.*, Phys. Lett. **B444**, 252 (1998).
[8] D. E. Gonzalez Trotter *et al.*, Phys. Rev. Lett. **83**, 3788 (1999).
[9] J. A. Nolen and J. P. Schiffer, Annu. Rev. Nucl. Sci. **19**, 471 (1969).
[10] K. Okamoto, Phys. Lett. **11**, 150 (1964).
[11] L. N. Epele, H. Fanchiotti, C. A. Garcia Canal, and G. A. Gonzalez Springberg, Phys. Lett. **B277**, 33 (1992).
[12] G. A. Miller, A. K. Opper, and E. J. Stephenson [nucl-ex/0602021].
[13] S. A. Coon and M. D. Scadron, Phys. Rev. C **26**, 562 (1982).
[14] Peter C. McNamee, Michael D. Scadron, and Sydney A. Coon, Nucl. Phys. **A249**, 483 (1975).
[15] S. A. Coon and M. D. Scadron, Nucl. Phys. **A287**, 381 (1977).
[16] P. G. Blunden and M. J. Iqbal, Phys. Lett. **B198**, 14 (1987).
[17] S. A. Coon and R. C. Barrett, Phys. Rev. C **36**, 2189 (1987).
[18] R. Machleidt and H. Müther, Phys. Rev. C **63**, 034005 (2001).
[19] T. D. Cohen and G. A. Miller, Phys. Rev. C **52**, 3428 (1995).
[20] J. Piekarewicz and A. G. Williams, Phys. Rev. C **47**, R2462 (1993).
[21] T. Goldman, J. A. Henderson, and A. W. Thomas, Few-Body Syst. **12**, 123 (1992).
[22] G. Krein, A. W. Thomas, and A. G. Williams, Phys. Lett. **B317**, 293 (1993).
[23] H. B. O'Connell, B. C. Pearce, A. W. Thomas, and A. G. Williams, Phys. Lett. **B336**, 1 (1994).
[24] S. A. Coon, B. H. J. McKellar, and A. A. Rawlinson, in *Intersections Between Particle and Nuclear Physics*, edited by T. W. Donelly, AIP Conf. Proc. No. 412 (AIP, Woodbury, NY, 1997), p. 368.
[25] T. Hatsuda, E. M. Henley, Th. Meissner, and G. Krein, Phys. Rev. C **49**, 452 (1994).
[26] A. K. Dutt-Mazumder, B. Dutta-Roy, and A. Kundu, Phys. Lett. **B399**, 196 (1997).
[27] W. Broniowski and W. Florkowski, Phys. Lett. **B440**, 7 (1998).
[28] A. K. Dutt-Mazumder, R. Hofmann, and M. Pospelov, Phys. Rev. C **63**, 015204 (2000).
[29] S. Zschocke and B. Kampfer, Phys. Rev. C **70**, 035207 (2004).
[30] P. Roy, A. K. Dutt-Mazumder, S. Sarkar, and J. Alam, J. Phys. G **35**, 065106 (2008).
[31] S. Biswas and A. K. Dutt-Mazumder, Phys. Rev. C **74**, 065205 (2006).
[32] Y. Mori and K. Saito, Phys. Lett. **B552**, 21 (2003).
[33] S. Biswas, P. Roy, and A. K. Dutt-Mazumder, Phys. Rev. C **78**, 045207 (2008).
[34] B. D. Serot and J. D. Walecka, Adv. Nucl. Phys. **16**, 1 (1986).
[35] S. A. Chin, Ann. Phys. (NY) **108**, 301 (1977).
[36] J. I. Kapusta, *Finite-Temperature Field Theory* (Cambridge University Press, New York, 1989).
[37] G. 'tHooft and M. T. Veltmann, Nucl. Phys. **B44**, 189 (1973).
[38] M. E. Peskin and D. V. Schroeder, *An Introduction to Quantum Field Theory* (Addision-Wesley, Reading, MA, 1995).
[39] T. P. Cheng and L. F. Li, *Gauge Theory of Elementary Particles* (Clarendon, New York, 2006).